Pharmaceutical Research, Vol. 24, No. 11, November 2007 (© 2007)
DOI: 10.1007/s11095-007-9369-2

Research Paper

Rapid Doxorubicin Efflux from the Nucleus of Drug-Resistant Cancer Cells Following Extracellular Drug Clearance

Vivien Y. Chen,[1] Maria M. Posada,[1] Lili Zhao,[1] and Gus R. Rosania[1,2]

Received March 8, 2007; accepted June 4, 2007; published online August 1, 2007

Purpose. Following extracellular drug clearance, we analyzed the rate of doxorubicin efflux from the nucleus of three human leukemic cells (K562, Molt4 and CCRF-CEM) and related it to their differential sensitivity to this drug, after a short drug pulse.
Results. For many pulse-chase regimes, K562 cell viability was least affected by doxorubicin. In K562 cells, nuclear drug accumulation was greatest, but nuclear drug egress was also greatest. P-glycoprotein over-expression in a doxorubicin-resistant, K562/DOX sub-line did not facilitate doxorubicin efflux from the nucleus. In K562 cells, doxorubicin accumulated in multivesicular bodies (MVBs) through a pH-dependent mechanism. Inhibiting drug sequestration in MVBs did not affect nuclear efflux. The rates of doxorubicin efflux from the nuclei of live and digitonin-permeabilized K562 cells were similar. However, extracting cytoplasmic membranes with Triton X-100 significantly inhibited nuclear drug efflux following extracellular drug clearance.
Conclusion. Our results are consistent with drug efflux from the nucleus being primarily mediated by an ATP-independent, passive diffusion mechanism. The effect of membrane extraction suggests that nonspecific drug absorption to cytoplasmic membranes plays a role in facilitating nuclear efflux in K562 cells, perhaps by lowering the concentration of free doxorubicin from a perinuclear diffusion boundary layer.

KEY WORDS: cellular pharmacokinetics; doxorubicin; drug delivery; drug resistance; drug sequestration; drug targeting; multivesicular body.

INTRODUCTION

Differences in intracellular accumulation and distribution of anticancer drugs in cancer cells may contribute to some cancer cells being less sensitive to chemotherapy than others. In this context, a new type of intrinsic drug resistance mechanism is of considerable interest: the efflux of cytotoxic drugs from the intracellular site of action, potentially facilitated by nonspecific drug absorption to membranes or sequestration in specific, membrane-bound organelles (1,2). In the cytoplasm of cancer cells, active transmembrane transport mechanisms can facilitate drug sequestration into lysosomes or endocytic vesicles (3), creating sink conditions in the cytosol after clearance of drug from the extracellular medium. Cytosolic sink conditions could facilitate drug unbinding from intracellular targets, contributing to decreased sensitivity of cancer cells to anticancer drugs.

In addition to active transport mechanisms, ion-trapping in low-pH compartments can mediate intracellular drug sequestration, to facilitate unbinding from the drug target (4). Weakly basic, hydrophobic drugs such as doxorubicin are neutral in cytosolic pH and can freely diffuse across membranes. Once they enter acidic compartments such as lysosomes, they become protonated and membrane-impermeant, so they can accumulate in acidic organelles (5,6). For example, daunorubicin predominantly accumulates in the nucleus, its site of action, in some drug-sensitive cell lines. In a drug-resistant sub-line of those cells, the drug is sequestered in cytoplasmic organelles, and this difference is associated with differences in the acidification of lysosomes (7).

K562 is a human erythroleukemic cell line that sequesters doxorubicin in cytoplasmic vesicles and is intrinsically more resistant to this drug, compared to other cell lines (8). K562 cells express low levels of MDR transporters and yet have the ability to survive anthracycline-induced cytotoxicity (9). MDR transporters can facilitate the intracellular drug sequestration in K562 and may contribute to the acquisition of multi-drug resistance (10). Biochemical analysis of intracellular doxorubicin concentration in K562 cells immediately following a drug pulse reveals that intracellular drug concentration is greater than extracellular concentration, yet doxorubicin continues to dissociate from the nucleus despite a large amount of intracellular drug (11). This observation can be explained by an intracellular sink condition in which doxorubicin is bound or otherwise compartmentalized, so there is little freely soluble doxorubicin in the cytosol. In K562 cells, doxorubicin efflux from the nucleus occurs at a faster rate in living cells compared to isolated nuclei,

[1] Department of Pharmaceutical Sciences, University of Michigan College of Pharmacy, 428 Church St., Ann Arbor, MI 48109, USA.
[2] To whom correspondence should be addressed. (e-mail: grosania@umich.edu)

0724-8741/07/1100-2156/0 © 2007 Springer Science + Business Media, LLC

suggesting the existence of a drug transport pathway facilitating nuclear efflux (12). Thus, while the cause of drug resistance is understood to be multi-factorial (13), intracellular drug sequestration may be one of the factors that can contribute to intrinsic drug resistance of K562 cells.

Here, we compare the viability of K562 leukemic cells in response to different doxorubicin pulse-chase treatments with that of other leukemic cell lines lacking intracellular sequestration mechanisms. Cytoplasmic drug sequestration in MVBs followed rapid nuclear efflux in K562 cells, and led to alterations of MVB morphology and increased numbers of MVBs. In K562 cells, MVBs appeared to fuse with the plasma membrane to facilitate exocytosis of drug. However, incubation of cells with ammonium chloride—an agent that raises the pH of acidic organelles—inhibited drug sequestration in MVBs, but did not interfere with rapid nuclear efflux. Most importantly, extraction of cytoplasmic membranes with Triton X-100 decreased the rate of drug efflux from the nucleus, but plasma membrane permeabilization with digitonin did not have such an effect. The digitonin experiment suggests that in K562 cells nuclear efflux may be facilitated by an ATP-independent mechanism. The Triton X-100 experiment suggests cytoplasmic membrane binding may be responsible—at least partly—for facilitating passive diffusion of doxorubicin molecules out of the nucleus.

MATERIALS AND METHODS

Cell Culture. K562, Molt4, and CCRF-CEM cells (National Cancer Institute, Bethesda, MD) were maintained in tissue culture medium (RPMI supplemented with 10% FBS and 1% penicillin/streptomycin at 37°C with 5% $C0_2$). K562/DOX cells were a gift from Dr. Duxin Sun (Ohio State University, Columbus, OH) and were maintained in tissue culture medium with once-monthly stimulation with 0.1 μM doxorubicin. All experiments were done with cells in logarithmic growth phase ($0.2–1.0 \times 10^6$ cells/ml).

Cell Viability Experiments. Cells were pulsed with 0.001–100 μM doxorubicin (Bedford Laboratories, Bedford, OH) in tissue culture medium for 10 min–4 h and then plated at a density of 20 K cells/well in 96-well plates. Viable cell populations after 0 and 48 h post wash-out of drug were assessed using the MTT cell proliferation assay according to the manufacturer's directions (ATCC, Manassas, VA). To calculate GI50 values, cell proliferation in treated cells was compared to untreated controls. The GI50 value is the drug concentration at which the increase in MTT-reducing activity of a drug-treated, cell population is inhibited by 50%, as compared to an untreated (control) cell population, over a 48 h period. Sigmoidal dose response curves were fit to the data using SigmaPlot (Systat Software Inc., Point Richmond, CA) and used to compute the GI50 for each experiment. The mean GI50 and SEM for each pulse-chase regimen and cell type were calculated from three separate experiments. To determine statistical significance, a one-tailed homoscedastic *t*-test was performed to calculate the *p* value.

Efflux Experiments. Cells were pulsed with 10–100 μM doxorubicin in RPMI for 1 h at 37°C. Following the pulse, cells were washed twice with fresh tissue culture medium and incubated in drug-free tissue culture medium for up to 4 h. Where indicated, the chase period was carried out in 10 mM NH_4Cl in RPMI. To analyze nuclear efflux in permeabilized cells, K562 cells were permeabilized with digitonin or Triton following a 1-h 100 μM doxorubicin pulse. For extraction using digitonin, cells were incubated with 60 μg/ml digitonin in intracellular buffer for 5 min on ice. Cells were then washed twice with buffer before being incubated in buffer at 37°C for 8 h. At the end of the efflux period, the nuclei of digitonin-permeabilized cells were isolated using Triton as described below. For extraction using Triton, cells were first permeabilized with digitonin as described above and then incubated in 1% Triton in intracellular buffer for 15 min and again washed twice before being incubated in buffer for 8 h. Control cells were pulsed with drug and then incubated in cell culture media at 37°C for 8 h. At the end of the efflux period, control cells were permeabilized with digitonin and then Triton so that all the cells went through the same extraction steps over the course of the experiment. To measure nuclear efflux in K562 versus K562/DOX cells, both cell types were pulsed with 100 μM doxorubicin in tissue culture medium for 1 h at 4°C. Cells were then washed with fresh media and incubated at 37°C for 4 h. To determine statistical significance, a one-tailed homoscedastic *t*-test was performed to calculate the *p* value.

Intracellular Drug Measurements. Drug mass in nuclei was determined as previously described (12). At the end of the efflux period, membrane and freely soluble drug were extracted by incubating cells in 1% Triton X-100 in intracellular buffer (30 mM HEPES, 10 mM EGTA, 0.5 mM EDTA, 5 mM magnesium sulfate and 33 mM potassium acetate; pH 7.4) for 15 min. Nuclear pellets were isolated after centrifugation at $1,000 \times g$ for 5 min. Nuclear pellets were washed twice and resuspended in buffer by vortexing. Samples comprised of 500–750 K nuclei in 100 μl of buffer were transferred to individual wells in 96-well plates, and data was acquired with a Typhoon 9200 fluorescence scanner (Amersham Biosciences, Piscataway, NJ). Doxorubicin fluorescence was captured with green laser illumination (535 nm) and the 580 BP 30 emission filter on the instrument. To normalize for cell number, the nucleic acid stain Syto 63 (Molecular Probes, Eugene, OR) was added to each well at the concentrations recommended by the manufacturer and imaged using red laser illumination (633 nm) and the 670 BP 30 emission filter. The 16-bit plate image data files were analyzed with Metamorph software (Molecular Devices Corporation, Sunnyvale, CA). Doxorubicin mass in each well was calculated using a standard curve of drug in buffer. In validation experiments, we established that the integrated fluorescence intensity and total doxorubicin mass exhibited a linear relationship across the range of experimental measurements, and that measurements were comparable before and after digesting the DNA and proteins in the samples using DNase I and Proteinase K. We also confirmed that the overall loss of cellular doxorubicin, as determined by the difference in the total drug mass within the cells before and after the efflux period, was comparable to the measured drug mass that accumulated in the extracellular medium during efflux. Therefore, we concluded that the binding of doxorubicin to cellular components did not impact its fluorescence measurement in our assay and could be quantitated using a standard of drug in buffer. The total number of cells in each

well was calculated using standard curves made by varying numbers of cells stained with Syto dye. In each well, dividing the total mass of doxorubicin by the number of nuclei yielded the mass of doxorubicin per nucleus. The mean nuclear drug mass and SEM for each cell type and time point were calculated from at least three separate experiments. To determine statistical significance, a one-tailed homoscedastic *t*-test was performed to calculate the *p* value.

Fluorescence Staining. For plasma membrane labeling, K562 cells were incubated with 4 μM FM1-43 (Molecular Probes) in ice-cold HBSS for up to 25 min according to the manufacturer's protocol. To track endocytosis, cells were incubated with 4 μM FM1-43 in tissue culture medium at 37°C for up to 1 h. For labeling of cytoplasmic membranes, K562, Molt4, and CCRF-CEM cells were first permeabilized with 60 μg/ml digitonin in PBS on ice for 5 min. The cells were then washed twice with PBS and incubated with 4 μM FM1-43 in PBS. FM1-43 fluorescence was captured with green laser illumination (535 nm) and the 526 SP emission filter on the fluorescence scanner. To label acidic compartments, K562 cells were incubated with 75 nM Lysotracker Green (Molecular Probes) in tissue culture medium for 30 min.

Microscopy. For confocal microscopy, cells were imaged with an Olympus FV-500 microscope (Olympus Corp., Center Valley, PA) using a 100× oil immersion objective. Argon laser (488 nm) illumination was used to acquire images of Lysotracker Green (LTG) or FM1-43, and a HeNe Green laser (543 nm) was used to acquire images of doxorubicin, in two separate detection channels. RGB color overlays were created with Adobe Photoshop from separate grey scale images, with the doxorubicin image in the R channel; LTG or FM1-43 image in the G; and black fill in the B. For electron microscopy, untreated and doxorubicin-pulsed K562 cells were washed twice with serum-free media, incubated at 37°C with 2.5% glutaraldehyde in 0.1 M Sorensen's buffer at pH 7.4 for 30 min, and washed twice with 0.1 M Sorensen's buffer. Samples were prepared for microscopy 8 h after a 1-h, 1–100 μM drug pulse and immediately after a 24-h, 0.5 μM doxorubicin pulse. Cells were fixed with 1% osmium tetroxide in 0.1 M Sorensen's buffer for 15 min at 4°C and washed three times with ddH_20. Uranyl acetate was added for a final concentration of 8%, and then cells were incubated for 1 h at room temperature. The sample was dehydrated in a graded ethanol/water series (50, 70, 90 and 100%) for 5 min each, and then infiltrated in Epon resin (Resolution Performance Products, Houston, TX) and polymerized at 60°C for 24 h. The stained cells were visualized and photographed with a Phillips CM/100 transmission electron microscope at magnifications from 3,600 to 130,000×.

RESULTS

Cell Viability is Greater in K562 than in Molt4 or CCRF-CEM Cells for Similar Doxorubicin Pulse-Chase Regimes

To determine doxorubicin's effect on cell viability following extracellular drug clearance, K562, Molt4, and CCRF-CEM cells were pulsed with 1 nM to 100 μM doxorubicin for 10 min to 4 h and then incubated in drug-free medium for 48 h. Cell viability after 48 h was determined using the MTT assay (14) and compared to the untreated control (Fig. 1a). Based on the MTT assay, CCRF-CEM cells were most sensitive to the drug. Molt4 cells had intermediate sensitivity. MTT reducing activity was least affected in K562 cells, at all concentrations and pulse lengths tested. GI50 values were calculated from the MTT assay (Fig. 1b). The GI50 values for K562 cells were three to 60-fold greater than the other cell lines for every pulse-chase regimen tested (mean p value < 0.02).

K562 Cells Accumulate more Nuclear Doxorubicin than Molt4 or CCRF-CEM When Pulsed with Drug, and Doxorubicin Exits the Nucleus More Rapidly

The decreased sensitivity of K562 cells to doxorubicin could be explained by a decrease in the rate of doxorubicin influx or an increase in the rate of doxorubicin efflux from the drug's site of action. Previously, we determined that the doxorubicin concentrations inside nuclei of K562 cells reach steady levels within 5 min after drug addition (12). Molt4 and CCRF-CEM cells were also found to establish steady-state nuclear drug concentrations within 5 min (data not shown). To test if differences in cell viability between the cell lines were due to differences in doxorubicin influx or to facilitated drug efflux from the nucleus, cells were pulsed with 10 μM doxorubicin for 1 h and then incubated in tissue culture media for 4 h to allow for drug efflux. Cell nuclei were isolated at the beginning and end of the efflux period, and the nuclear drug mass was determined. The amount of drug in the nucleus was significantly higher immediately following the pulse in K562 cells as compared to the other cells (p value < 0.004; Fig. 2a). After 4 h under efflux conditions, the drug mass in the nuclei of K562 cells had decreased by more than 30%, a significantly greater amount (p value < 0.03) than Molt4 and CCRF-CEM cells, both of which exhibited <10% loss in nuclear drug content (Fig. 2b). Thus, doxorubicin efflux from the nucleus is fastest in K562 cells. This is consistent with this cell line's increased viability in every pulse-chase regime tested. Because nuclear drug mass in K562 cells is greater than in the other cell lines following exposure to doxorubicin, the reduced growth inhibitory activity of doxorubicin in K562 cells cannot be ascribed to its inability to reach the target.

K562 Cells—but not Molt4 or CCRF-CEM—Sequester Doxorubicin in Cytoplasmic Vesicles

Drug sequestration in cytoplasmic organelles has been proposed to be a mechanism facilitating nuclear efflux (15). To test if this may explain the higher rate of nuclear efflux in K562 cells relative to the other cell lines, cells were pulsed with 10 μM doxorubicin for 1 h and then imaged using a confocal microscope after 4 h under efflux conditions (Fig. 3). K562 cells exhibited nuclear localization of doxorubicin, as well as sequestration of the drug in cytoplasmic vesicles. Molt4 and CCRF-CEM cells exhibited drug localization in the nucleus only. Previously, we observed that drug accumulation in cytoplasmic vesicles of K562 cells occurs gradually under efflux conditions (12). Given that steady-state drug concentrations within nuclei are established within 5 min for

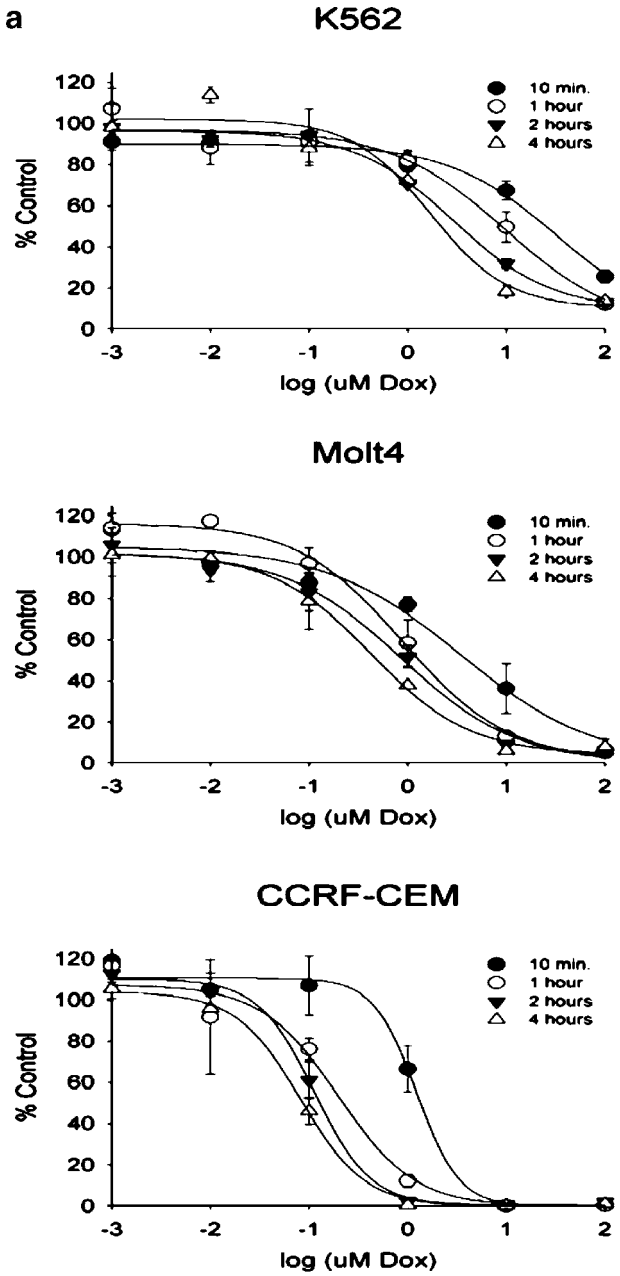

b

	GI50 (uM)		
Pulse Time	K562	Molt4	CCRF
10 minutes	33.10 ± 2.09	3.17 ± 0.56	1.30 ± 0.23
1 hour	8.86 ± 1.93	0.92 ± 0.30	0.15 ± 0.03
2 hours	3.19 ± 0.82	0.85 ± 0.12	0.12 ± 0.02
4 hours	1.54 ± 0.30	0.43 ± 0.03	0.08 ± 0.01

◀ **Fig. 1.** K562 cells are intrinsically more resistant to doxorubicin than Molt4 and CCRF-CEM. **a** Cell viability determined using the MTT assay in treated cells compared to the untreated control after cells were pulsed with 0.001 to 100 μM doxorubicin for 10 min to 4 h. **b** GI50 values calculated for the different pulse lengths for each cell line. Data are the means of three experiments ± SEM.

all cell lines (12), drug sequestration following extracellular drug clearance is most closely associated with nuclear efflux, as observed in K562 cells.

Doxorubicin-Sequestering Cytoplasmic Vesicles Belong to the Endocytic Pathway

In a previous study (12), we found evidence that in K562 cells, doxorubicin accumulates in organelles that morphologically resemble multivesicular bodies of the endo-lysosomal compartment. To confirm that the organelles accumulating doxorubicin in K562 cells correspond to this endo-lysosomal compartment, cells were pulsed with 10 μM doxorubicin and then labeled with the styryl dye FM1-43, and imaged using a confocal microscope (Fig. 4). FM1-43 is used as a fluorescent marker of endocytosis (16) because the dye is lipophilic and partitions preferentially at the plasma membrane before gradually accumulating in intracellular endocytic vesicles through endocytosis of the plasma membrane. In K562 cells, FM1-43 initially only labeled the plasma membrane (Fig. 4), with doxorubicin mostly present in the nucleus and cytoplas-

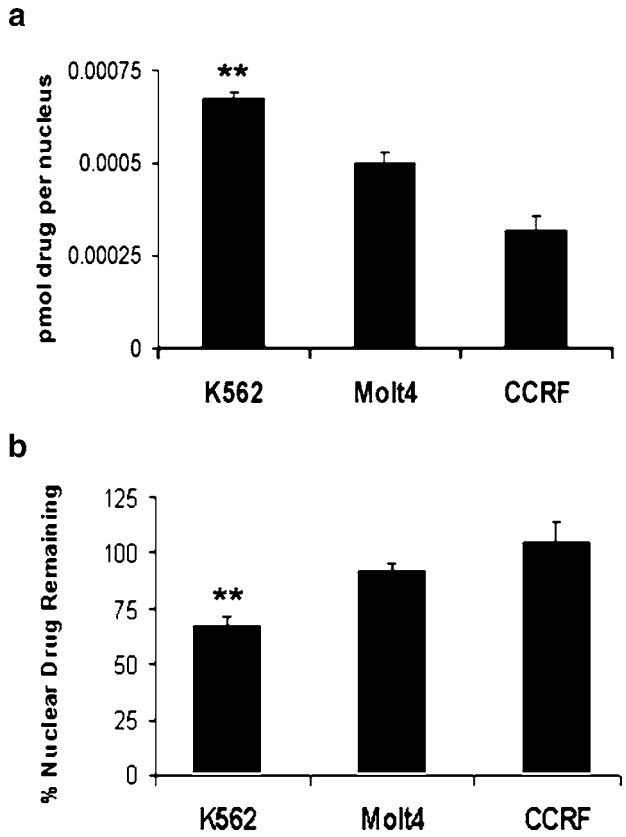

Fig. 2. K562 cells accumulate more doxorubicin in the nucleus and have a facilitated nuclear efflux mechanism. **a** Mass of doxorubicin per nucleus immediately following a 1-h 10 μM drug pulse. **b** Percentage of the initial drug mass remaining in the nucleus after 4 h under efflux conditions. Data are the means of three experiments ± SEM. The *double asterisks* denote statistical significance (p value < 0.05).

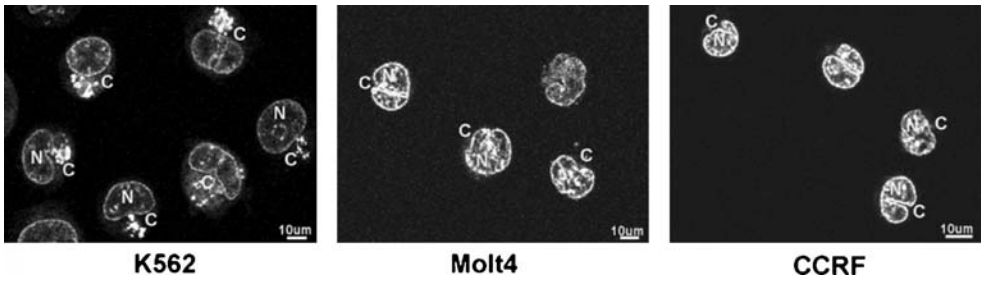

Fig. 3. K562 cells sequester doxorubicin in cytoplasmic vesicles. Confocal images of K562, Molt4, and CCRF-CEM cells 2 h after a 1-h 10 μM doxorubicin pulse (*N* denotes the nucleus, and *C* denotes the cytoplasm).

mic vesicles. After longer incubation times, which allowed for the endocytosis of FM1-43, co-localization between doxorubicin and FM1-43 in cytoplasmic vesicles became increasingly visible (Fig. 4). After 1 h of incubation, large doxorubicin-containing intracellular vesicles were also labeled with FM1-43 (Fig. 4). These results provide evidence that the intracellular doxorubicin-containing vesicles correspond to late endosomes or lysosomes, which is consistent with our previous report indicating that in K562 cells, doxorubicin accumulates in intracellular vesicles that correspond in size, number and location to MVBs (12).

Doxorubicin-laden Cytoplasmic Vesicles of K562 Cells can Fuse with the Plasma Membrane

In K562 cells, MVBs are known to undergo fusion with the plasma membrane, releasing the intralumenal vesicles of the MVBs into the extracellular medium (17). These intralumenal vesicles are known as "exosomes". Generally, exosomes are shed from cells upon fusion of MVBs with the plasma membrane and serve as a disposal route for monoubiquitinated membrane proteins (18). To determine if doxorubicin-sequestering organelles in K562 cells are able to fuse with the plasma membrane, K562 cells were pulsed with 100 μM doxorubicin for 1 h. After an 8-h chase period in drug-free medium, the cells were labeled with FM1-43. The incubation with FM1-43 was brief (<25 min) and carried out in ice-cold buffer to halt endocytosis. Confocal microscope images showed some large doxorubicin-containing vesicles adjacent to the plasma membrane labeled with FM1-43 (Fig. 5), while the doxorubicin-containing vesicles located further from the plasma membrane remained unlabeled. Since FM1-43 does not penetrate the plasma membrane and is nonfluorescent in aqueous media, the bright labeling of such vesicles indicates fusion of the doxorubicin-containing vesicles with the plasma membrane. It also indicates a high lipid content in the doxorubicin-containing vesicles. These results are consistent with previous observations of FM1-43 staining of exosome-loaded MVBs fusing with the plasma membrane (19).

The Number and Morphology of MVBs Changes in Response to Doxorubicin

Following up on these experiments, we tested if drug sequestration in MVBs affected the structure or function of this organelle. For this purpose, transmission electron microscopy was used to monitor the number, size and

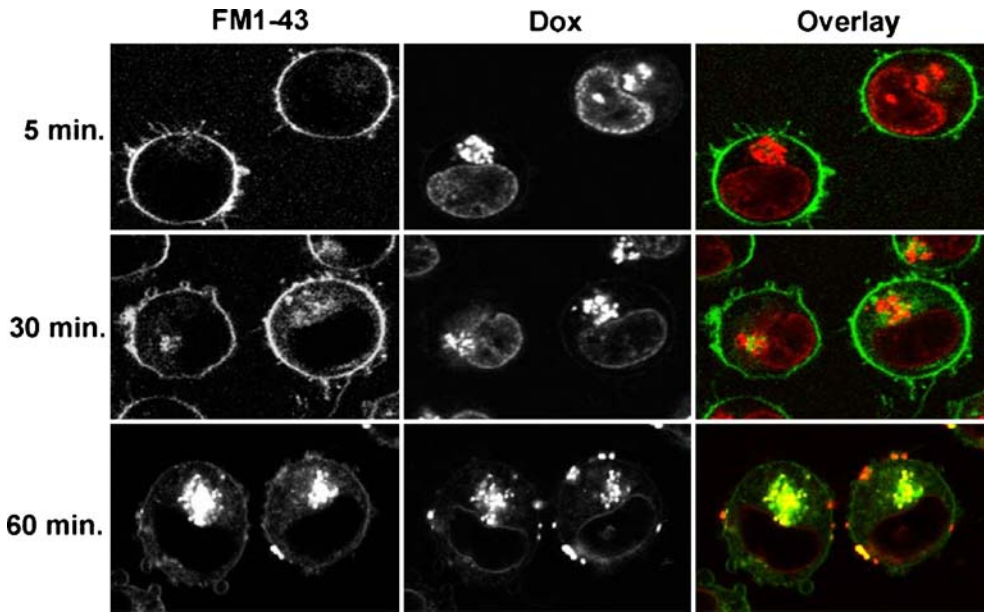

Fig. 4. Doxorubicin is sequestered in endocytic compartments of K562 cells. Confocal images of doxorubicin and FM1-43, 4 h after a 1-h 10 μM drug pulse. Cells were incubated with FM1-43 for 5 min to 1 h. The *left column* shows FM1-43 distribution. The *middle column* shows doxorubicin localization. The *right column* is an overlay of these two images.

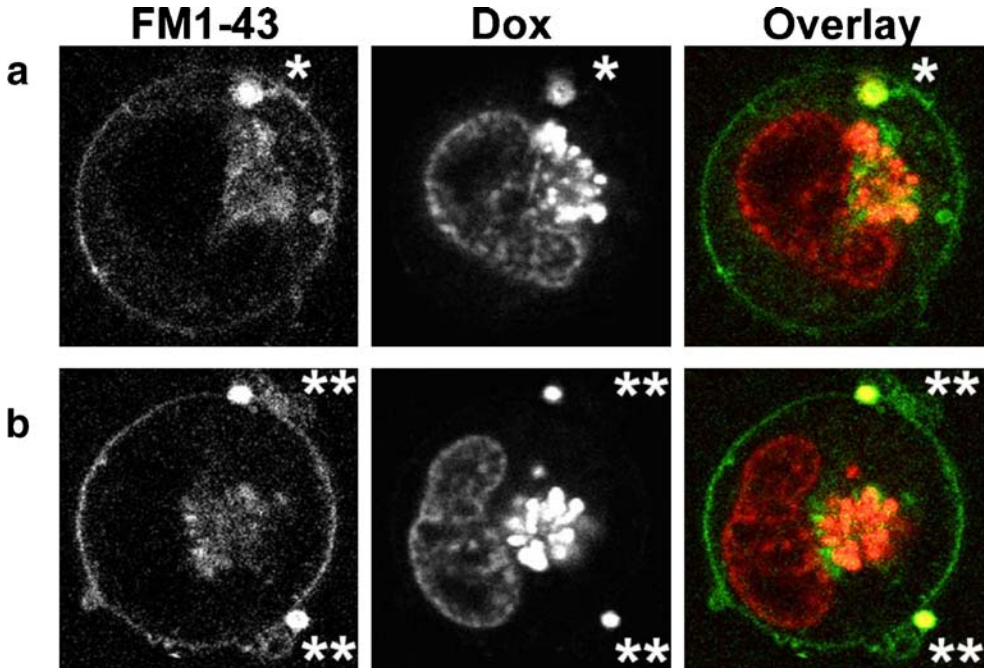

Fig. 5. Doxorubicin-containing vesicles of K562 cells fuse with the plasma membrane. Confocal images of doxorubicin and FM1-43 in K562 cells 8 hours after a 1-hour 100 μM drug pulse. The cells were briefly incubated with FM1-43 to selectively label the plasma membrane and any membraneous compartments exposed to the extracellular medium. The *left column* shows FM1-43 distribution. The *middle column* shows doxorubicin localization. The *right column* is an overlay of these two images. **a** A cell containing a doxorubicin and FM1-43 labeled vesicle in the cytoplasmic side of the plasma membrane (*single asterisk*). **b** A cell containing two doxorubicin and FM1-43 labeled vesicles in the extracellular side of the plasma membrane (*double asterisk*). Note that several vesicles in the cytoplasm are labeled with doxorubicin alone, as FM1-43 is largely confined to the plasma membrane.

morphology of MVBs in K562 cells treated with doxorubicin. In untreated K562 cells, numerous small vesicles could be seen in the lumen of the MVBs (Fig. 6a). Cells treated with a short, 1-h pulse of 1 to 10 μM doxorubicin contained MVBs with morphologies similar to the control, but with several slightly enlarged intralumenal vesicles (Fig. 6b, c). Cells pulsed for 24 h with 0.5 μM doxorubicin (Fig. 6d), and cells pulsed with 100 μM doxorubicin for 1 h (Fig. 6e) both exhibited enlarged intralumenal vesicles of varying size in the MVBs. Furthermore, the MVBs assumed irregular morphologies and sometimes appeared as multilamellar structures (data not shown). Counting the frequency of MVBs revealed an increase in the number of cells containing MVBs and the number of MVBs per cell (Fig. 6f) after doxorubicin treatment. In comparison, the number and morphology of other organelles remained largely unaffected (data not shown). Thus, doxorubicin exposure appeared to exert specific effects on MVBs consistent with drug accumulation in the organelle.

NH_4Cl Inhibits Cytoplasmic Doxorubicin Sequestration, But Not Efflux from the Nucleus

NH_4Cl is a lysosomotropic, membrane-permeant weak base that serves as a proton-shuttle, dissipating transmembrane pH gradients and thus raising lumenal endo-lysosomal pH (20). By this mechanism, NH_4Cl inhibits sequestration of weakly basic molecules in lysosomes and is commonly used to test the role of ion-trapping in drug sequestration in acidic organelles (21–23). To determine if ion-trapping in acidic vesicles is a mechanism of doxorubicin sequestration in K562 cells, K562 cells were pulsed with 10 μM doxorubicin for 1 h and labeled with the control molecule Lysotracker Green (LTG) (24) after 2 h of efflux time. Confocal microscope images showed colocalization of the drug and LTG in cytoplasmic vesicles, indicating that doxorubicin accumulated in acidic compartments (Fig. 7a). When the experiment was carried out in the presence of NH_4Cl, cytoplasmic sequestration of doxorubicin and LTG was markedly decreased. To compare the effect of NH_4Cl on nuclear efflux of drug, cells were pulsed with doxorubicin and then incubated in drug-free media with and without 10 mM NH_4Cl for 4 h. Both control cells and NH_4Cl-treated cells demonstrated a similar loss in nuclear doxorubicin (Fig. 7b). Thus, despite inhibiting drug sequestration, NH_4Cl treatment did not significantly affect nuclear drug efflux.

Extraction of Intracellular Membranes, But Not Plasma Membrane Permeabilization, Inhibits Nuclear Efflux of Doxorubicin

The effects of plasma membrane permeability and cytoplasmic membranes in nuclear efflux were investigated in cells treated with digitonin and Triton X-100. In the control cells, both the plasma membrane and cytoplasmic membranes were intact, resulting in the sequestration of doxorubicin and LTG in cytosolic vesicles and exclusion of Trypan Blue (Fig. 8a). Digitonin permeabilized the plasma membrane, allowing for Trypan Blue staining, but preserved the integrity of the internal membranes so that Lysotracker still accumulated intracellularly (Fig. 8a). Neither LTG nor

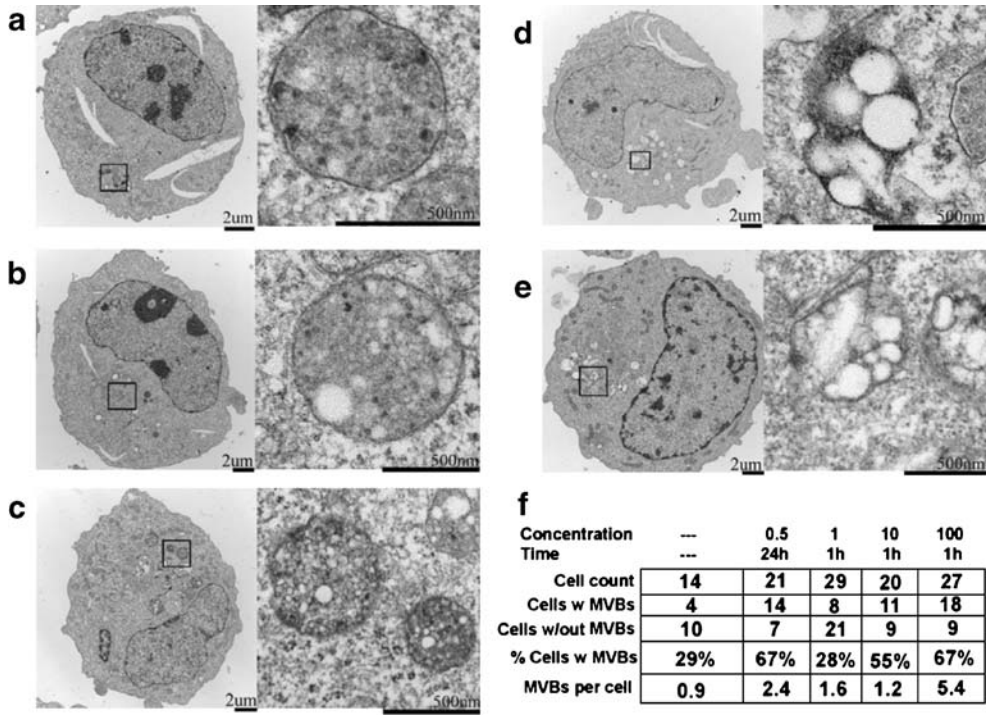

f

Concentration	---	0.5	1	10	100
Time	---	24h	1h	1h	1h
Cell count	14	21	29	20	27
Cells w MVBs	4	14	8	11	18
Cells w/out MVBs	10	7	21	9	9
% Cells w MVBs	29%	67%	28%	55%	67%
MVBs per cell	0.9	2.4	1.6	1.2	5.4

Fig. 6. Doxorubicin induces morphological changes in MVBs of K562 cells. Electron micrographs at 5,800× magnification (*left panel*) and a representative MVB from each cell at 13,500× magnification (*right panel*), after: **a** no treatment; **b** a 1-h 1 μM drug pulse and 8-h efflux period; **c** a 1-h 10 μM drug pulse and 8-h efflux period; **d** A 24-h 0.5 μM drug pulse; **e** a 1-h 100 μM drug pulse and 8-h efflux period; **f** quantitative summary of microscopic observations indicate how doxorubicin increases both the number of MVBs per cell and the fraction of cells with MVBs.

doxorubicin became sequestered in cytosolic compartments after digitonin treatment, which was not surprising since permeabilizing the plasma membrane would be expected to induce leakage of intracellular ATP. Without ATP, the H^+-ATPase maintaining the acidic pH of endo-lysosomal vesicles would not function. In contrast, Triton X-100 extraction removed all the cytoplasmic cellular membranes so that neither doxorubicin nor LTG fluorescence was visible outside the nucleus (Fig. 8a). Nuclear efflux of drug in intact cells and permeabilized cells were compared (Fig. 8b). After a 1-h 100 μM drug pulse and 8 h under efflux conditions, Triton-extracted cells lost significantly less doxorubicin (p value < 0.002) than intact or digitonin-permeabilized cells. Intact cells and digitonin-extracted cells exhibited a loss of 35–40% of the initial nuclear drug mass, while Triton-extracted cells lost less than 20% of the nuclear doxorubicin acquired during the pulse period. The difference in nuclear efflux between Triton- and digitonin-permeabilized cells suggested that intracellular membranes may facilitate nuclear efflux. The similar rate of drug egress in intact and digitonin-extracted cells indicated that soluble cytosolic components such as ATP, which would be released following plasma membrane perforation, may not be essential for rapid nuclear efflux to occur.

K562 Cells Bind More FM1-43 to Cytoplasmic Membranes than CCRF-CEM Cells, But Binding is Comparable Between K562 and Molt4 Cells

K562, Molt4, and CCRF-CEM cells were permeabilized using digitonin and then incubated with FM1-43 to assess cytoplasmic membrane content. The extent of FM1-43 binding to membranes was examined using confocal microscopy and a fluorescence imager to quantitate fluorescence intensity (Fig. 9). The cytoplasmic membrane mass stained with FM1-43 was visibly larger and brighter in K562 and Molt4 cells compared to CCRF-CEM (Fig. 9a). The intensity of FM1-43 fluorescence per cell was determined to be comparable in K562 and Molt4 cells (Fig. 9b), however the amount of FM1-43 bound to CCRF-CEM cells was significantly lower (p value $< 6.0\text{E-}9$). That CCRF-CEM cells exhibit the least FM1-43 staining is consistent with the slow rate of nuclear drug efflux and increased sensitivity to doxorubicin observed for this cell line.

K562 and K562/Dox Cells Exhibit Similar Rates of Nuclear Efflux of Doxorubicin

Nuclear efflux of doxorubicin in K562 and the drug-resistant sub-line K562/Dox cells were compared to determine the potential role of the drug transporter P-glycoprotein (P-gp) in nuclear efflux (Fig. 10). P-gp is highly induced in K562/DOX cells, with 600-fold greater expression of MDR1 mRNA compared to K562 cells (25). At 37°C, K562/DOX cells accumulate much less doxorubicin in the nucleus, compared to the parent cell line (data not shown). Therefore, to measure nuclear efflux of doxorubicin, K562 and K562/DOX cells were pulsed with doxorubicin for 1 h at 4°C, to inactivate P-gp and allow for comparable starting concentrations of drug in the nucleus in both cell types (Fig. 10b). Following the pulse, cells were incubated at 37°C to allow for

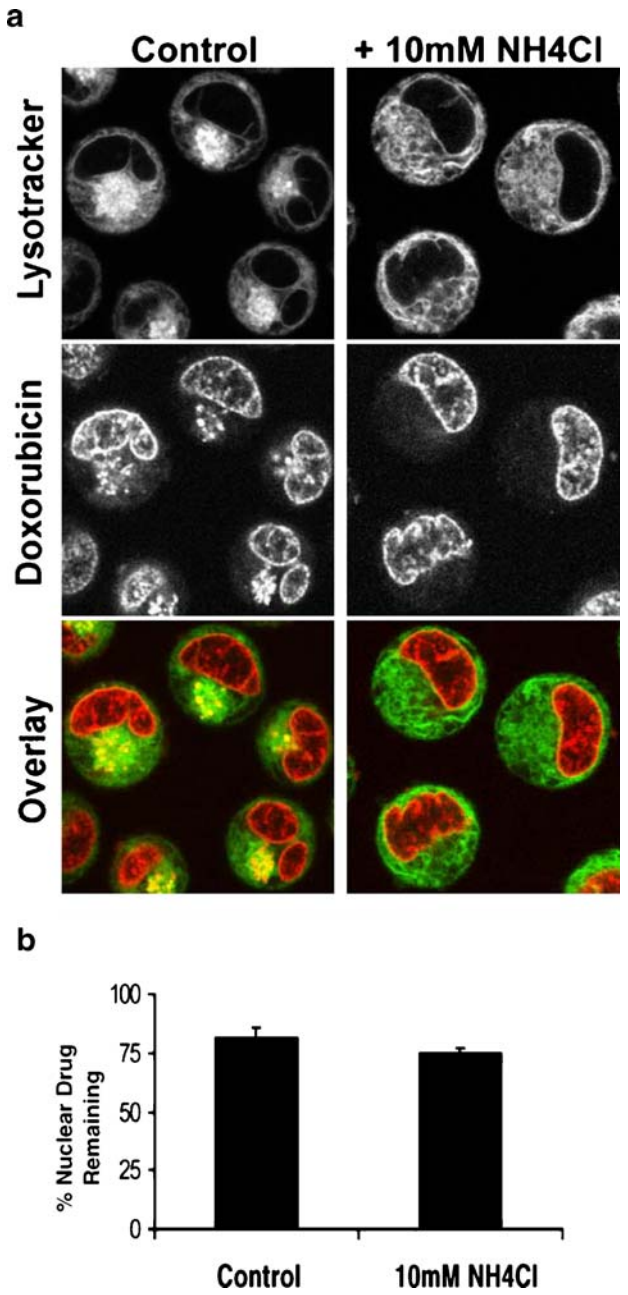

Fig. 7. Increasing vesicular pH abolishes drug sequestration in K562 cells, but nuclear efflux can still occur. **a** Confocal images of doxorubicin and Lysotracker Green localization in cells following a 1-h 100 μM drug pulse and 2 h efflux. The *left column* shows control cells and the *right column* shows cells that were incubated with 10 mM NH_4Cl following the pulse. The *top row* shows Lysotracker distribution. The *middle row* shows doxorubicin localization. The *bottom row* is an overlay of these two images. **b** Percentage of the initial drug mass remaining in the nucleus after a 1-h 100 μM drug pulse and 4 h under efflux conditions in the presence and absence of 10 mM NH_4Cl. Data are the means of three experiments ± SEM.

recovery of normal cell function. Confocal images taken of isolated nuclei showed similar levels of doxorubicin fluorescence intensity in both K562 and K562/DOX cells before and after the efflux period (Fig. 10a). After 4 h under efflux conditions, K562 and K562/DOX cells lost comparable amounts of nuclear drug, with both cell types exhibiting a significant loss (p value < 0.003) of 45–55% of the starting doxorubicin mass (Fig. 10b). The similar rates of nuclear egress in K562 and K562/DOX cells suggest that differences in plasma membrane permeability (or drug transporter overexpression) do not account for differences in the rates of drug efflux from the nucleus.

DISCUSSION

The Pathway of Drug Efflux from the Nucleus Varies in Cells Differentially Sensitive to Doxorubicin

Generally, the sensitivity of cancer cells to anticancer agents is assessed in the presence of a constant extracellular drug concentration (26). The extent to which these methods of assaying anticancer drug activity are relevant to the activity of anticancer drugs in vivo might depend on whether clearance of extracellular drug is a factor affecting the response of tumor cells to anticancer agents. Once an anticancer drug is injected into the bloodstream, its concentration steadily decreases. For example, doxorubicin once injected intravenously distributes rapidly and extensively into

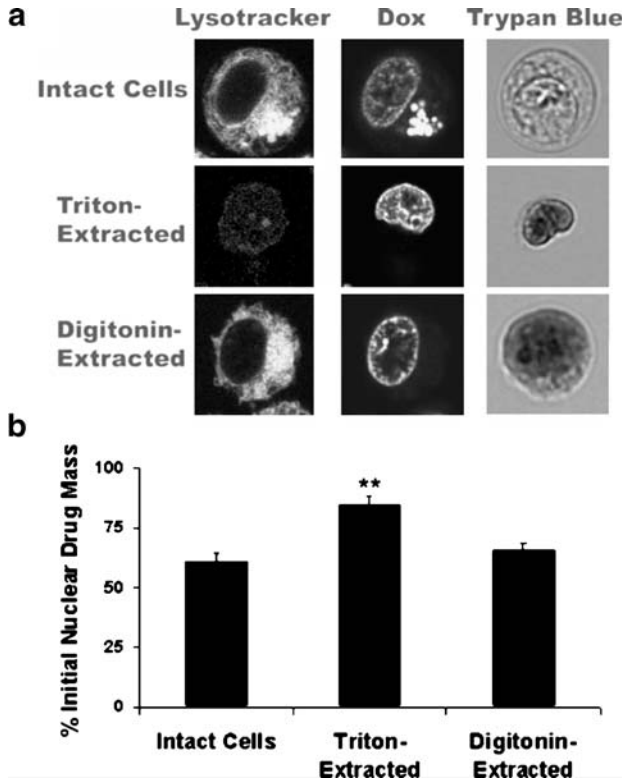

Fig. 8. Nuclear efflux of drug is inhibited by extraction of intracellular membranes, but not permeabilization of the plasma membrane. **a** Images of doxorubicin, Lysotracker Green (LTG), and Trypan Blue localization in intact cells and cells permeabilized with digitonin and Triton. The *left column* shows LTG localization, the *middle column* shows doxorubicin distribution, and the *right column* shows Trypan Blue staining. The *top row* shows control, unpermeabilized cells. The *middle row* shows Triton-extracted cells, and the *bottom row* shows digitonin-extracted cells. **b** Percentages of the initial nuclear drug mass remaining after a 100 μM drug pulse and 8 h under efflux conditions. Data are the means of six experiments ± SEM. The *double asterisk* denotes statistical significance (p value < 0.002).

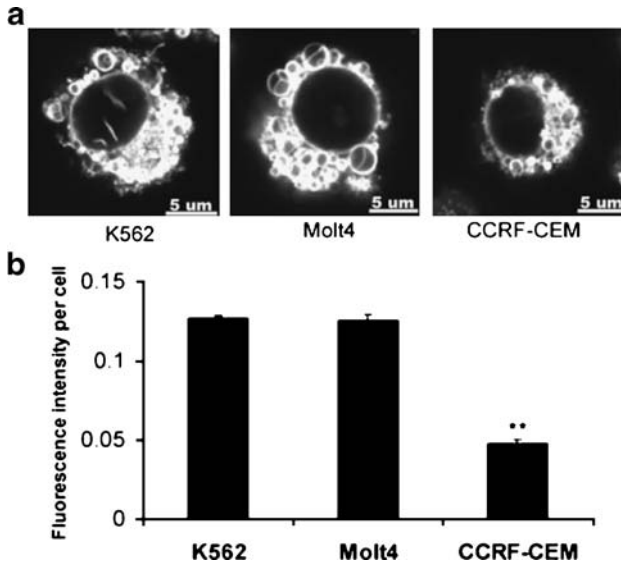

Fig. 9. K562 and Molt4 cells have significantly greater cytoplasmic membrane content than CCRF-CEM cells. **a** Images of FM1-43 labeled intracellular membranes in digitonin-permeabilized cells. **b** FM1-43 fluorescence intensity per cell measured using a fluorescence imager. Data are the means of four experiments ± SEM. The *double asterisk* denotes statistical significance (p value < 6.0E-9).

tissues (27). The remaining free drug is metabolized by the liver, eliminated by biliary excretion, and bound to plasma proteins (28). Previous studies have shown that less than 2% of the injected doxorubicin dose accumulates in tumors (29,30). Thus, systemic drug concentrations seldom remain constant after drug administration.

In the present study, the response of several human leukemic cell lines to anticancer agents was monitored in pulse-chase experiments. Under these conditions, K562 cells are less sensitive to doxorubicin than Molt4 or CCRF-CEM cells (Fig. 1). One possible explanation for this difference could be that K562 cells accumulate less doxorubicin in the nucleus during the pulse period. However, doxorubicin uptake during the pulse period is actually greatest in K562 cells (Fig. 2a). Most importantly, the nuclear doxorubicin content decreases in K562 cells during the chase period, while it stays almost constant in other cell lines (Fig. 2b). This suggests a facilitated nuclear efflux pathway in K562 cells. Interestingly, of the three cell lines, K562 are the only cells that visibly sequester doxorubicin in cytoplasmic vesicles (Fig. 3), indicating that cell viability, rapid nuclear efflux and drug sequestration in cytoplasmic vesicles may be related.

One can hypothesize that, as doxorubicin unbinds from DNA in K562 cells, free doxorubicin diffuses to the cytoplasm, where it immediately binds to membranes, by nonspecific absorption. More gradually, it becomes sequestered into an acidic, late endo-lysosomal compartment such as an MVB. Inside MVBs are exosomes, membranous vesicles that are actively secreted by K562 cells through the fusion of MVBs with the plasma membrane (17). Shed vesicles have previously been implicated as a mechanism of doxorubicin expulsion from cancer cells (31). At acidic pH, doxorubicin is positively charged so it can absorb to negatively charged phospholipids of the exosome membrane, through both hydrophobic partitioning and electrostatic interaction (32,33). Incubating cells with NH_4Cl, an agent that raises lysosomal pH by dissipating pH gradients across membranes, abolishes sequestration of doxorubicin in MVBs (Fig. 7a). In MVBs, doxorubicin sequestration into MVBs may be driven by a combination of ion-trapping of the protonated form of the drug, together with adsorption of doxorubicin molecules to the inner membranes of the multivesicular or multilamellar body. This dual mechanism may explain why the concentration of doxorubicin in an endo-lysosomal compartment may be greater than expected from a purely ion-trapping mechanism (34).

Consistent with doxorubicin sequestration in MVBs, the number and morphology of MVBs change in cells incubated with the drug (Fig. 6). It is possible that doxorubicin sequestration alters organelle morphology by interfering with the mechanism that leads to the invagination of the MVB membrane (35) or by binding to exosomes (31). Multilamellar organelles have been observed in other cell types exposed to weakly basic, lysosomotropic drugs, a phenotype referred to as drug-induced phospholipidosis (36). Electron microscopy and colocalization of doxorubicin fluorescence with VPS4a-GFP (a GFP-tagged protein that marks MVBs) constitute additional evidence that doxorubicin accumulates in MVBs of K562 cells (12).

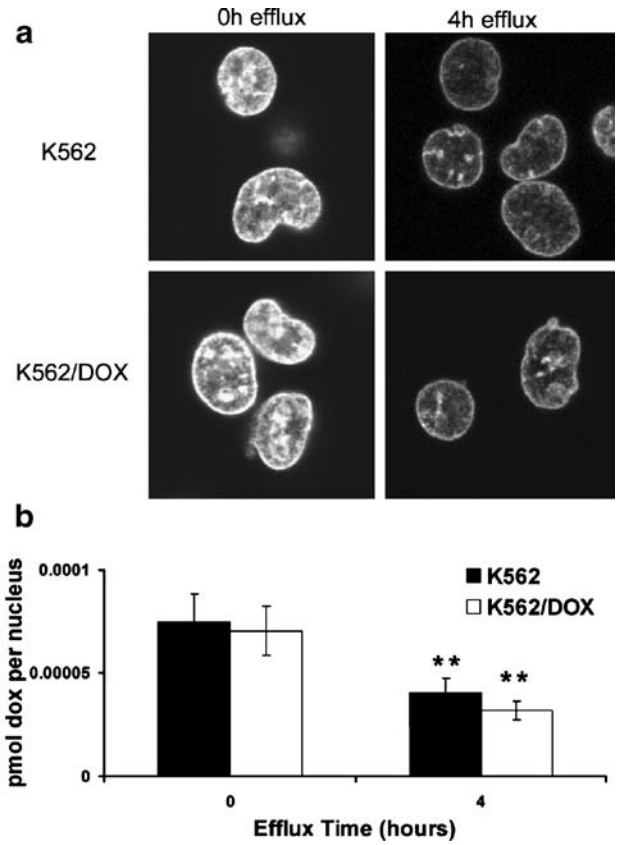

Fig. 10. K562 and K562/DOX cells exhibit similar rates of nuclear efflux of drug. **a** Images of doxorubicin fluorescence in nuclei isolated from K562 and K562/DOX cells following a 100 μM drug pulse at 4°C, before and after 4 h under efflux conditions at 37°C. **b** Nuclear drug mass per cell immediately following the doxorubicin pulse and 4 h post wash-out of drug. Data are the means of three experiments ± SEM. The *double asterisk* denotes statistical significance (p value < 0.003).

In K562 cells double-labeled with doxorubicin and a brief pulse of the styryl dye FM1-43, doxorubicin-sequestered organelles in close proximity to the plasma membrane became labeled with FM1-43, while the organelles deep inside the cell were unlabeled (Fig. 5). This indicates that doxorubicin-loaded MVBs near the plasma membrane may actually fuse with the plasma membrane and release their contents to the extracellular medium. In independent studies, multivesicular bodies have also been reported to undergo plasma membrane fusion (37,38). Prolonged incubation allows for the endocytosis of FM1-43, and colocalization of doxorubicin and FM1-43 further supports that the drug is sequestered in endocytic compartments (Fig. 4).

ATP-Dependent Mechanisms Do Not Account for Facilitated Nuclear Efflux of Doxorubicin in K562 Cells

Evidence for a facilitated drug efflux mechanism from the nucleus of K562 cells first came from experiments indicating that the amount of doxorubicin associated with the nuclei of K562 cells decreased at a faster rate in living cells than in isolated nuclei (12). Comparing the doxorubicin content of Molt4 and CCRF-CEM cells with that of K562 cells pulsed with drug and then chased in drug-free medium indicates differences in the rate at which doxorubicin exits the nucleus in different cell lines (Fig. 2). We hypothesized the existence of a nuclear drug efflux mechanism upregulated in K562 cells. As a topoisomerase II inhibitor, the interaction of doxorubicin with DNA is directly involved in the drug's primary mechanism of action. Therefore, a specific mechanism facilitating drug unbinding from DNA in K562 cells might also explain the observed differences in cell viability in the different cell lines (Fig. 1).

Although K562 was the only cell line of the three that visibly sequestered doxorubicin in cytoplasmic organelles (Fig. 3), abolishing sequestration through the pH-dependent, ion-trapping mechanism did not inhibit the rate of drug efflux from the nucleus (Fig. 7b). This indicates that a nuclear efflux mechanism able to operate independently of MVB sequestration may serve to facilitate efflux, which is consistent with reports of other cellular components acting upstream from MVBs to mediate drug transport between the nucleus and cytoplasm (39,40). Probing other ATP-dependent biological mechanisms that could potentially affect the rate of nuclear efflux, we found that although nuclear uptake of doxorubicin in P-gp overexpressing K562/DOX cells is reduced relative to the parent K562 cells, the rate that doxorubicin exits the nucleus in K562 and drug-resistant K562/DOX cells is comparable (Fig. 10). Therefore, while P-gp can keep doxorubicin from entering the cell, perhaps by preventing plasma membrane associated molecules from diffusing into the cytosol, its effect on drug clearance from the nuclear site of action is minimal.

ATP-Independent, Rapid Nuclear Efflux Occurs in Digitonin-Permeabilized K562 Cells

From experiments comparing the nuclear efflux rate in digitonin-permeabilized cells to intact cells, it appears that an ATP-independent mechanism may facilitate drug egress from the nucleus of K562 cells (Fig. 8). Although plasma membrane permeabilization should allow for efflux of ATP and other small molecules from the cell (also making them permeable to Trypan Blue in the extracellular buffer; Fig. 8), nuclear egress of drug in such cells was comparable to that of intact, viable cells. This indicated that differences in nuclear efflux rates in different cell lines may be influenced by physicochemical variables affecting doxorubicin unbinding from DNA or diffusion out of the nucleus. Digitonin-extracted cells retain their cytoplasmic membranes, as evident from their ability to bind the lipophilic styryl dye FM1-43 (Fig. 9). In contrast, Triton-extracted cells are devoid of cytoplasmic membranes (evident from reduced FM1-43 binding (data not shown) and lack of LTG staining; Fig. 8). Triton-extracted cells exhibited significantly slower nuclear efflux of drug than digitonin-permeabilized cells. The rate of nuclear efflux in digitonin-permeabilized cells demonstrates that cell viability is not essential for rapid drug transport out of the nucleus, and that nuclear egress can occur even when ATP has leaked out from the cell. The inhibition of drug efflux from the nucleus following Triton X-100 extraction suggests a role for cytoplasmic membranes in facilitating diffusion of drug away from the nucleus.

One possible explanation for the difference in the rate at which drug unbinds from the nucleus in the presence and absence of perinuclear membranes may directly involve the depletion of free doxorubicin molecules from the nuclear vicinity by nonspecific drug absorption to membranes (32,33). As doxorubicin molecules unbind from DNA, a diffusion boundary layer of doxorubicin molecules can form around the nucleus and slow down the rate of drug unbinding from DNA, by providing a high local concentration of free drug molecules around the DNA that would drive the forward reaction of the drug-DNA interaction. The observation that nuclear efflux occurs at a similar rate in K562 cells when cytoplasmic membranes are intact (even when drug does not become compartmentalized into MVBs) suggests that drug absorption to membranes may be sufficient to facilitate nuclear efflux. Therefore, although ion-trapping of doxorubicin in MVBs may contribute to depletion of free drug molecules in the cytosol and their excretion via an exocytic mechanism, it may not be the primary mechanism facilitating nuclear efflux.

The question remains whether differences in cytoplasmic membrane content explain differences in nuclear efflux rates amongst leukemic cell lines. K562 cells differ from CCRF-CEM cells in their cytoplasmic membrane content and display significantly more FM1-43 binding (Fig. 9). Together with differences in nuclear surface area due to a larger size of K562 cells (data not shown), this may help to explain the faster rate of nuclear egress of drug in K562 vs CCRF-CEM cells. However, K562 and Molt4 cells do not have obvious differences in perinuclear membrane content or in cell size that could explain the differences in nuclear efflux rates. Thus, there must be another explanation for the slower rate of drug efflux from the nuclei of Molt4 cells.

CONCLUSION

To our knowledge, the present study is the first to consider mechanisms potentially facilitating doxorubicin efflux from the nucleus in relation to differences in cell

viability following extracellular drug clearance. Our observations support the existence of a facilitated nuclear drug efflux pathway in K562 cells, relative to other leukemic cell lines. We hypothesize that this mechanism may be partly responsible for promoting the viability of K562 cells exposed to doxorubicin, as the ability of cells to clear nuclear doxorubicin would most certainly promote their survival after drug exposure. Only in K562 cells is doxorubicin visibly sequestered in organelles, forming MVBs that may facilitate cellular drug clearance. However, inhibiting MVB sequestration with ammonium chloride—or plasma membrane permeabilization with digitonin—did not slow down drug egress from the nucleus, supporting an ATP-independent, diffusion mechanism primarily responsible for facilitating doxorubicin efflux.

ACKNOWLEDGEMENTS

We thank Dr. Duxin Sun and Seth Gibbs and for the K562/DOX cells. This work was funded by grants from the National Institutes of Health (R21-CA104686 and R01-GM078200 to G.R.R.). V.Y.C. was supported by a Pre-Doctoral Fellowship from the Pharmaceutical Research and Manufacturers of America Foundation and a Pharmacological Sciences Training Program grant from the National Institute of General Medical Sciences (GM07767). Contents are solely the responsibility of the authors and do not necessarily represent the official views of NIGMS.

REFERENCES

1. R. Safaei, B. J. Larson, T. C. Cheng, M. A. Gibson, S. Otani, W. Naerdemann, and S. B. Howell. Abnormal lysosomal trafficking and enhanced exosomal export of cisplatin in drug-resistant human ovarian carcinoma cells. *Mol. Cancer Ther.* **4**:1595–1604 (2005).
2. Y. Gong, M. Duvvuri, M. B. Duncan, J. Liu, and J. P. Krise. Niemann-Pick C1 protein facilitates the efflux of the anticancer drug daunorubicin from cells according to a novel vesicle-mediated pathway. *J. Pharmacol. Exp. Ther.* **316**:242–247 (2006).
3. A. Rajagopal and S. M. Simon. Subcellular localization and activity of multidrug resistance proteins. *Mol. Biol. Cell* **14**:3389–3399 (2003).
4. V. Y. Chen and G. R. Rosania. The great multidrug-resistance paradox. *ACS Chem. Biol.* **1**:271–273 (2006).
5. C. de Duve, T. de Barsy, B. Poole, A. Trouet, P. Tulkens, and F. Van Hoof. Commentary. Lysosomotropic agents. *Biochem. Pharmacol.* **23**:2495–2531 (1974).
6. F. Rashid, R. W. Horobin, and M. A. Williams. Predicting the behaviour and selectivity of fluorescent probes for lysosomes and related structures by means of structure-activity models. *Histochem. J.* **23**:450–459 (1991).
7. Y. Gong, M. Duvvuri, and J. P. Krise. Separate roles for the Golgi apparatus and lysosomes in the sequestration of drugs in the multidrug-resistant human leukemic cell line HL-60. *J. Biol. Chem.* **278**:50234–50239 (2003).
8. L. Wu, A. M. Smythe, S. F. Stinson, L. A. Mullendore, A. Monks, A. Scudiero, K. D. Paull, A. D. Koutsoukos, L. V. Rubinstein, and M. R. Boyd. Multidrug-resistant phenotype of disease-oriented panels of human tumor cell lines used for anticancer drug screening. *Cancer Res.* **52**:3029–3034 (1992).
9. P. Ferrao, P. Sincock, S. Cole, and L. Ashman. Intracellular P-gp contributes to functional drug efflux and resistance in acute myeloid leukaemia. *Leuk. Res.* **25**:395–405 (2001).
10. V. Noskova, P. Dzubak, G. Kuzmina, A. Ludkova, D. Stehlik, R. Trojanec, A. Janostakova, G. Korinkova, V. Mihal, and M. Hajduch. In vitro chemoresistance profile and expression/function of MDR associated proteins in resistant cell lines derived from CCRF-CEM, K562, A549 and MDA MB 231 parental cells. *Neoplasma* **49**:418–425 (2002).
11. H. Tapiero, G. Nguyen-Ba, and T. J. Lampidis. Cross resistance relevance of the chemical structure of different anthracyclines in multidrug resistant cells. *Pathol. Biol.* **42**:328–337 (1994).
12. V. Y. Chen, M. M. Posada, L. L. Blazer, T. Zhao, and G. R. Rosania. The role of the VPS4A-exosome pathway in the intrinsic egress route of a DNA-binding anticancer drug. *Pharm. Res.* **23**:1687–1695 (2006).
13. S. M. Simon and M. Schindler. Cell biological mechanisms of multidrug resistance in tumors. *Proc. Natl. Acad. Sci. U S A* **91**:3497–3504 (1994).
14. T. Hayon, A. Dvilansky, O. Shpilberg, and I. Nathan. Appraisal of the MTT-based assay as a useful tool for predicting drug chemosensitivity in leukemia. *Leuk. Lymphoma.* **44**:1957–1962 (2003).
15. D. Marquardt and M. S. Center. Drug transport mechanisms in HL60 Cells isolated for resistance to adriamycin: evidence for nuclear drug accumulation and redistribution in resistant cells. *Cancer Res.* **52**:3157–3163 (1992).
16. W. J. Betz, F. Mao, and C. B. Smith. Imaging exocytosis and endocytosis. *Curr. Opin. Neurobiol.* **6**:365–371 (1996).
17. A. Savina, M. Vidal, and M. I. Colombo. The exosome pathway in K562 cells is regulated by Rab11. *J. Cell. Sci.* **115**:2505–2515 (2002).
18. D. J. Katzmann, G. Odorizzi, and S. D. Emr. Receptor down-regulation and multivesicular-body sorting. *Nat. Rev. Mol. Cell. Biol.* **3**:893–905 (2002).
19. A. F. Fomina, T. J. Deerinck, M. H. Ellisman, and M. D. Cahalan. Regulation of membrane trafficking and subcellular organization of endocytic compartments revealed with FM1-43 in resting and activated human T cells. *Exp. Cell Res.* **291**:150–166 (2003).
20. S. Ohkuma and B. Poole. Fluorescence probe measurement of the intralysosomal pH in living cells and the perturbation of pH by various agents. *Proc. Natl. Acad. Sci. U S A* **75**:3327–3331 (1978).
21. J. Ishizaki, K. Yokogawa, M. Hirano, E. Nakashima, Y. Sai, S. Ohkuma, T. Ohshima, and F. Ichimura. Contribution of lysosomes to the subcellular distribution of basic drugs in the rat liver. *Pharm. Res.* **13**:902–906 (1996).
22. C. Millot, J. M. Millot, H. Morjani, A. Desplaces, and M. Manfait. Characterization of acidic vesicles in multidrug-resistant and sensitive cancer cells by acridine orange staining and confocal microspectrofluorometry. *J. Histochem. Cytochem.* **45**:1255–1264 (1997).
23. W. A. Daniel, J. Wojcikowski, and A. Palucha. Intracellular distribution of psychotropic drugs in the grey and white matter of the brain: the role of lysosomal trapping. *Br. J. Pharmacol.* **134**:807–814 (2001).
24. T. Haller, P. Dietl, P. Deetjen, and H. Volkl. The lysosomal compartment as intracellular calcium store in MDCK cells: a possible involvement in InsP3-mediated Ca2+ release. *Cell Calcium* **19**:157–165 (1996).
25. L. Fang, G. Zhang, C. Li, X. Zheng, L. Zhu, J. Xiao, G. Szakacs, J. Nadas, K. K. Chan, P. G. Wang, and D. Sun. Discovery of a daunorubicin analogue that exhibits potent antitumor activity and overcomes P-gp-mediated drug resistance. *J. Med. Chem.* **49**:932–941 (2006).
26. M. Page. High-volume screening. In B. A. Teicher (ed), *Anticancer Drug Development Guide*, Humana, Totowa, 1997, pp. 3–21.
27. P. A. Speth, Q. G. van Hoesel, and C. Haanen. Clinical pharmacokinetics of doxorubicin. *Clin. Pharmacokinet.* **15**:15–31 (1988).
28. F. M. Balis, J. S. Holcenberg, and W. A. Bleyer. Clinical pharmacokinetics of commonly used anticancer drugs. *Clin. Pharmacokinet.* **8**:202–232 (1983).
29. J. Vaage, E. Barbera-Guillem, R. Abra, A. Huang, and P. Working. Tissue distribution and therapeutic effect of intravenous free or encapsulated liposomal doxorubicin on human prostate carcinoma xenografts. *Cancer* **73**:1478–1484 (1994).
30. D. W. Northfelt, F. J. Martin, P. Working, P. A. Volberding, J. Russell, M. Newman, M. A. Amantea, and L. D. Kaplan. Doxorubicin encapsulated in liposomes containing surface-

bound polyethylene glycol: pharmacokinetics, tumor localization, and safety in patients with AIDS-related Kaposi's sarcoma. *J. Clin. Pharmacol.* **36**:55–63 (1996).
31. K. Shedden, X. T. Xie, P. Chandaroy, Y. T. Chang, and G. R. Rosania. Expulsion of small molecules in vesicles shed by cancer cells: association with gene expression and chemosensitivity profiles. *Cancer Res.* **63**:4331–4337 (2003).
32. D. A. Tyrrell, T. D. Heath, C. M. Colley, and B. E. Ryman. New aspects of liposomes. *Biochim. Biophys. Acta* **457**:259–302 (1976).
33. E. Goormaghtigh, P. Chatelain, J. Caspers, and J. M. Ruysschaert. Evidence of a specific complex between adriamycin and negatively-charged phospholipids. *Biochim. Biophys. Acta* **597**:1–14 (1980).
34. M. Duvvuri and J. P. Krise. A novel assay reveals that weakly basic model compounds concentrate in lysosomes to an extent greater than pH-partitioning theory would predict. *Mol. Pharm.* **2**:440–448 (2005).
35. M. Babst. A protein's final ESCRT. *Traffic* **6**:2–9 (2005).
36. N. Anderson and J. Borlak. Drug-induced phospholipidosis. *FEBS Lett.* **580**:5533–5540 (2006).
37. B. T. Pan, K. Teng, C. Wu, M. Adam, and R. M. Johnstone. Electron microscopic evidence for externalization of the transferrin receptor in vesicular form in sheep reticulocytes. *J. Cell Biol.* **101**:942–948 (1985).
38. G. Raposo, H. W. Nijman, W. Stoorvogel, R. Liejendekker, C. V. Harding, C. J. Melief, and H. J. Geuze. B lymphocytes secrete antigen-presenting vesicles. *J. Exp. Med.* **183**:1161–1172 (1996).
39. T. A. Chan, H. Hermeking, C. Lengauer, K. W. Kinzler, and B. Vogelstein. 14-3-3Sigma is required to prevent mitotic catastrophe after DNA damage. *Nature* **401**:616–620 (1999).
40. K. Kiyomiya, S. Matsuo, and M. Kurebe. Mechanism of specific nuclear transport of adriamycin: the mode of nuclear translocation of adriamycin-proteasome complex. *Cancer Res.* **61**:2467–2471 (2001).